QUANTUM COMPUTING IN FOUR SPATIAL DIMENSIONS

Arturo Tozzi (Corresponding author)
Center for Nonlinear Science, University of North Texas
1155 Union Circle, #311427
Denton, TX 76203-5017 USA
tozziarturo@libero.it
Arturo.Tozzi@unt.edu

Muhammad Zubair Ahmad
Department of Electrical and Computer Engineering
University of Manitoba
Winnipeg, Canada
ahmadmz@myumanitoba.ca

James F. Peters
Department of Electrical and Computer Engineering, University of Manitoba
75A Chancellor's Circle
Winnipeg, MB R3T 5V6 CANADA
James.Peters3@umanitoba.ca

Relationships among near set theory, shape maps and recent accounts of the Quantum Hall effect pave the way to quantum computations performed in higher dimensions. We illustrate the operational procedure to build a quantum computer able to detect, assess and quantify a fourth spatial dimension. We show how, starting from two-dimensional shapes embedded in a 2D topological charge pump, it is feasible to achieve the corresponding four-dimensional shapes, which encompass a larger amount of information. This novel, relatively straightforward architecture not only permits to increase the amount of available qbits in a fixed volume, but also converges towards a solution to the problem of optical computers, that are not allowed to tackle quantum entanglement through their canonical superposition of electromagnetic waves.

KEYWORDS: Hall effect; oscillations; fourth dimension; computer; superlattice.

Multidimensional approaches are a novel field of research, with a potential to provide insights into physical and biological organization. However, it is currently technically demanding to cope with these elusive multidimensional activities. The recent onset of datasets encompassing thousands of features has led to the development of novel tools, such as feature selection, to model the underlying high-dimensional settings of data generation (Garcia et al., 2018). Despite feature selection techniques allow the reduction of the data dimensionality and improve algorithms' performance (Dmochowski et al., 2017), huge data volume makes learning tasks computationally demanding. Increasing features' quantity/complexity results in reduced computational efficiency of algorithms. Most of the algorithms in use, developed for datasets of small size, cannot cope with the emerging Big Data problems. Therefore, novel tools are required to quantify multidimensional issues related to mathematical, physical and biological systems. In quantum computing, quantum properties can be used to represent and structure data (stored in terms of qbits), providing an amount of information higher than the classical computers. Here we describe a novel quantum computing tool that is able, starting from simple shapes traces encompassed in a two-dimensional lattice, to detect information from a fourth spatial dimension. We aim to transfer the framework of the quantum Hall effects provided by Lohse et al. (2018) to the realm of quantum computing, to demonstrate the feasibility of a synthetic quantum network equipped with four spatial dimensions (plus time), instead of the classical three (plus time).

We will describe 4D quantum computing in terms of a computational device able to cope with *shape maps*, i.e., shapes' assessment at various hierarchical levels of synthesis. At first, we will define the fundamental structure for maps construction; then we will provide the operational steps for achieving 4D quantum computing. We will also show that shape maps provide an expanded view of the Borsuk-Ulam Theorem (Tozzi et al., 2017) which allows to increase the amount of available qbits.

INTRODUCING SHAPE MAPS

In near set theory, we consider a space K and a probe function $\phi: 2^K \to \mathbb{R}^n$ (Peters, 2007; Peters 2014). Given a a small neighborhood $U \subset K$, we construct the fiber bundle $(K_\Phi, K, \pi, \phi(U))$. Here K_Φ is termed the ***glossa*** (a set paired with description (Ahmad, Peters, 2018)), i.e., a space where each $k \in K$ is paired with $\phi(k)$, due to the local trivialization property. This structure can be described as follows:

$$\phi(U) \to K_\Phi \overset{\pi}{\to} K.$$

To define classical set theoretic operations incorporating description, we introduce the notion of ***descriptive intersection*** (Di Concilio et al., 2018). Let $A, B \subset K$ and $\phi: 2^K \to \mathbb{R}^n$. A descriptive intersection is defined as:

$$A \bigcap_\Phi B = \{x \in A \cup B: \phi(x) \in \phi(A) \ and \ \phi(x) \in \phi(B)\}.$$

Note that a descriptive intersection of sets A, B consists of all the elements. in either A or B, having the same description. It follows that all the elements in $A \cap B$ are included in the descriptive intersection. We can represent this definition in terms of fiber bundle structure and classical set theoretic operations as follows:

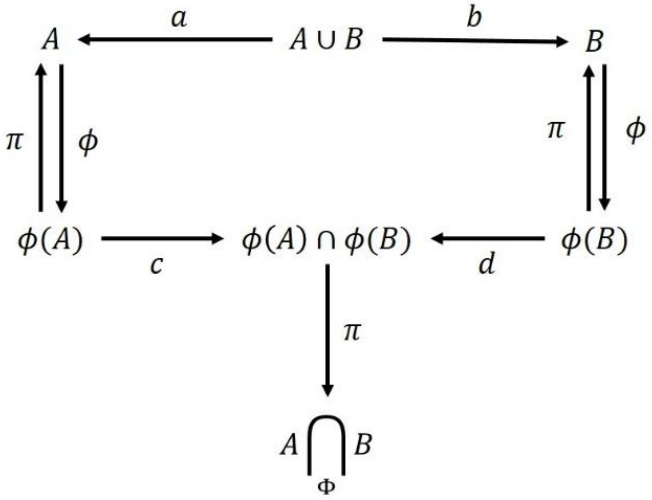

Once established the notion of descriptive intersection, the next step is to define a descriptive union. Four different possible definitions have been discussed by Ahmad and Peters (2018): they consider either elements in $A \cup B$(non-restrictive), or $A \cap B$(restrictive), or few values of description (descriptive discriminatory), or all possible values (descriptive nondiscriminatory). Here we will evaluate just the ***non-restrictive and descriptive discriminatory union***. Given $A, B \subset K$ and $\phi: 2^K \to \mathbb{R}^n$, non-restrictive and descriptive discriminatory union is described as follows:

$$A \bigcup_{\phi=\{i,j\}} B = \{x \in A \cup B: \phi(x) = i \ or \ \phi(x) = j\}.$$

A non-restrictive and descriptive discriminatory union of sets A,B consists of all the elements of A and B that have matching description values {i,j}, decided *a priori.* A more detailed account of the properties of this union is given

in Ahmad and Peters (2018). In terms of classical set theoretic operations and fiber bundles, the latter definition can be described in the following terms:

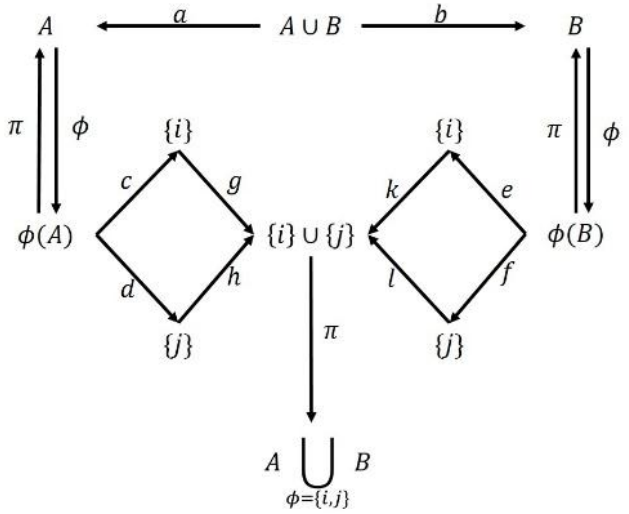

Shapes in terms of synthesis. The next step is to define representation of a shape as a synthesis. We begin with a set of shapes $\{Sh_i\}_{i\in\mathbb{Z}}$ with no description attached to them. For simplicity, we assume them as embedded in a 2-dimensional space. This set of shapes is said to be at synthesis level 0, which is represented as S_0. To attach description to these shapes, we use a probe function $\phi_1: 2^{S_0} \to \mathbb{R}^n$ at level 0 and achieve a glossa represented as $\{Sh_i \to \phi_1(Sh_i)\}_{i\in\mathbb{Z}}$, standing for the synthesis level 1 or S_1. We move onto the next level of synthesis, attaching another description to the one already attached in S_1. Thus, S_2 is constructed using a probe function $\phi_2: 2^{S_1} \to \mathbb{R}^n$. The corresponding glossa can be represented as $\{Sh_i \to \phi_1(Sh_i) \to \phi_2(\phi_1(Sh_i))\}_{i\in\mathbb{Z}}$. We generalize for the m^{th} synthesis level S_m, using the probe function $\phi_m: 2^{S_m} \to \mathbb{R}^n$. This means that the glossa at S_m can be written as $\{Sh_i \to \phi_1(Sh_i) \to \cdots \to \phi_{m-1}(\cdots \phi_1(Sh_i)) \to \phi_m(\phi_{m-1} \cdots \phi_1(Sh_i))\}_{i\in\mathbb{Z}}$. In sum, we define a family of functions that can be collectively termed as ***shape maps***. Let $s_i^{i+1}: S_i \to S_{i+1}$, be a map between the synthesis levels, then for a shape representation with m synthesis levels the shape maps are $\mathbb{S}_m = \{s_i^{i+1}\}_{i=1,2,\cdots,m-1}$.

Figure 1A shows a shape map encompassing different levels of synthesis. The shapes Sh_i, exist at S_0 the zeroth level of synthesis. At S_1, descriptions are attached to each shape with the help of a probe function ϕ_1. At the next level of synthesis, a description is attached to the description of each of the objects by ϕ_2. Similarly, increasing the levels of synthesis, we increase the number of descriptions until, at S_n, a description is attached to the previous level using ϕ_n. At the highest level, the description can be written as a composition of maps $\phi_n(\phi_{n-1} \cdots \phi_1(Sh_i))$.

Once achieved shapes representation with the desired level of synthesis, we need to "organize" them according to a general description throughout all the levels. By "organizing" we mean clustering the shapes into sets based on some similarity criterion. Here the previously described near set paradigm comes into play. For this purpose, the descriptive intersection (Di Concilio et al., 2018) and the non-restrictive and descriptive discriminatory union (Ahmad and Peters 2018) are used. It is noteworthy there just one descriptive intersection is feasible, while the number of non-restrictive and descriptive discriminatory union depends on the number of pairs of descriptions $\{i, j\}$ selected *a priori*. We have set of descriptive set theoretic operators for each S_m. Let us represent this set at synthesis level j as:

$$\mathcal{O}^j = \left\{ \bigcap_{\Phi}, \left\{ \bigcup_{\phi=A_i\in A} \right\}_{i\in\mathbb{Z}} \right\}, where\ A = \left\{x \in 2^{\boldsymbol{Codomain}(\phi_j)} : |x| = 2\right\}.$$

In this set, we achieve both descriptive intersection and a selection of the possible non-restrictive and descriptive discriminatory unions. Further, if we take into account any of these operators for S_i, the synthesis assesses the descriptions attached at S_i and provides again the elements of the S_{i-1} level. This is clear from the arrow diagrams

illustrated in **Figure 1A**, which show how the descriptive set theoretic operations return the elements in the base space K, rather than the ones in the glossa K_Φ. We assume that each of the operators in $\mathcal{O}^j$ can be used for a single set, instead of canonical binary operator. The same applies for the descriptive union in which all the elements with a priori decided descriptions are returned. We define a family of maps, which clusters the elements in S_i based on the application of operators in $\mathcal{O}^i$:

$$\mathcal{C}_i = \left\{c_j^i = s_{i-1}^i(\mathcal{O}_j^i(S_{i-1}))\right\}_{j=1,2,\cdots,|\mathcal{O}^i|} \text{ where, } \mathcal{O}_j^i \text{ is the } j^{th} \text{ element of the set } \mathcal{O}^i.$$

This map clusters the elements in S_i based on some similarity measure. If we consider the non-restrictive and descriptive discriminatory union with $\phi = \{i, j\}$ as the similarity measure, then it results in clustering all the shapes with description value of either i or j. Every operator in $\mathcal{O}^i$ results in a different cluster (set) of $S_i$elements. Because each $c_j^i: S_{i-1} \rightarrow S_i$, their union to form $\mathcal{C}_i$ results in a new space $P(S_i)$, built by clustering the $S_i$elements. Hence, we can represent this as $\mathcal{C}_i: S_{i-1} \rightarrow P(S_i)$. An example of this map is illustrated in **Figure 1B**. This Figure also illustrates the beginning of a hyper Borsuk-Ulam Theorem (Borsuk, 1957-58; Matoušek 2003; Tozzi and Peters 2016a). The introduction of a hyper-BUT paves the way to techniques for shape detection, "bunching" (clustering), classification, building (disparate shapes are synthesized to form new shapes for future reference), and shape analysis in a high-dimensional space (Tozzi and Peters 2016). Shape building, also called bulk building, allows new shapes to be achieved. The hierarchical view of shape maps leads to two forms of synthesis, namely, shape-gluing (descriptive intersection) and shape agglomeration (descriptive union). We define another family of maps for synthesis level m represented as $\mathfrak{C}_m = \{C_i\}_{i=1,2,\cdots m}$, termed ***clustering maps***. This allows to build a diagram termed ***shape description diagram***, illustrated in **Figure 1C**.

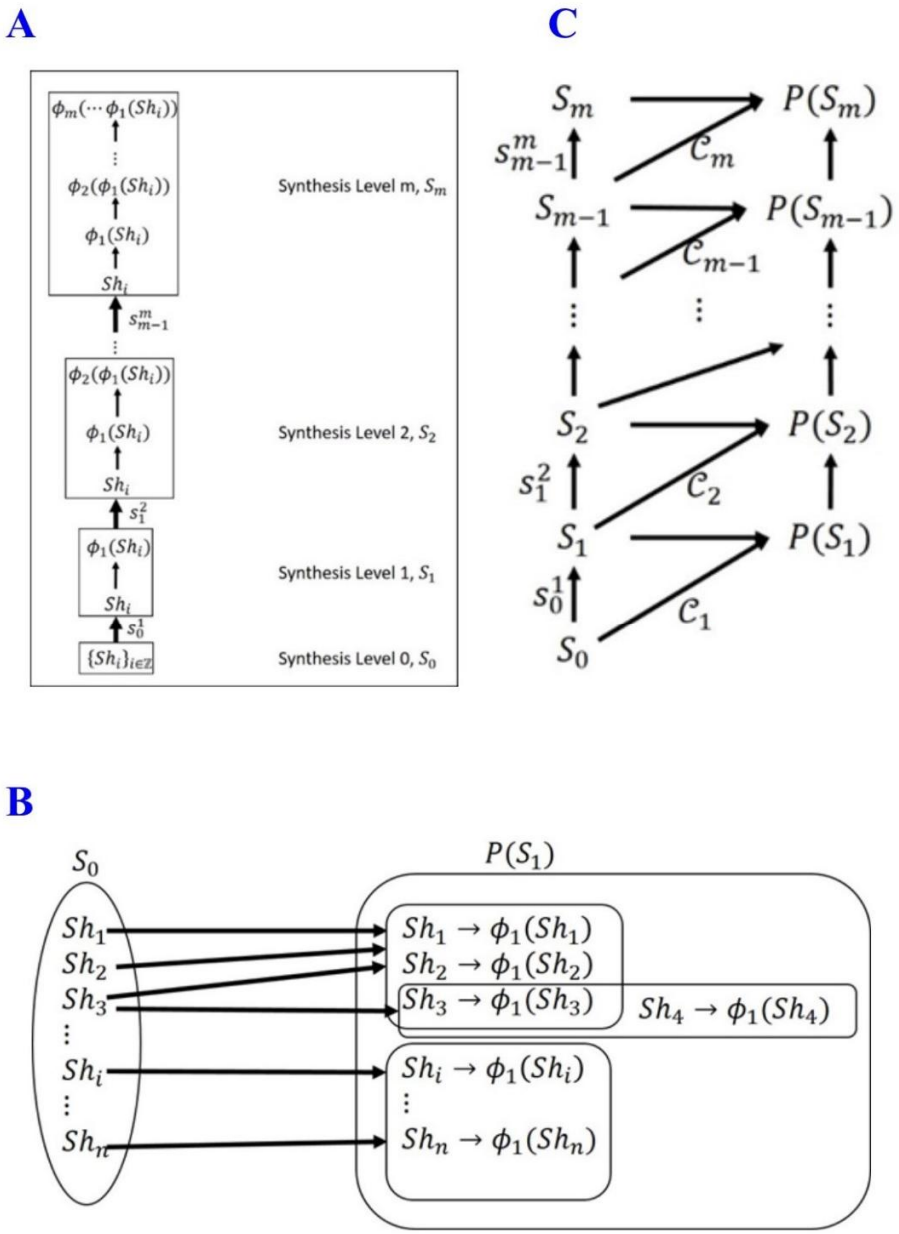

Figure 1. Topological steps of shape maps' construction. **Figure 1A**: shape maps with n-levels of synthesis. **Figure 1B**: shape maps lead to shapes clustered and glued together using descriptive intersection. **Figure 1C**: shape description diagram for m-synthesis levels. See text for further details.

A TOOL FROM THEORETICAL PHYSICS

Here we ask: is it feasible to assess and quantify how quantum oscillations may generate multidimensional computations? More specifically, is it feasible to build a real or an artificial oscillatory network able to simulate an otherwise undetectable fourth spatial dimension? The answer is affirmative. Recent experimental findings describe a technique that throws an operational bridge between theoretical physics and quantum computing. At first, we explore the "Hall effect" (Hall, 1879), *i.e.*, the production of potential difference transverse to electric current, upon application of a magnetic field perpendicular to current. Magnetic fields with the proper angulation are able to bend electric rays. A comparable phenomenon, called "quantum Hall effect", occurs in quantum dynamics (Novoselov et al., 2007). An electric charge sandwiched between two surfaces behaves like a two-dimensional material: when this material is cooled down to near absolute-zero temperature and subjected to a strong magnetic field, the amount that it can conduct becomes "quantized", leading to the so-called quantum Hall effect (Tozzi, 2019). This puzzling phenomenon is easily explained, if we take into account that it occurs in four, instead of the canonical three, spatial dimensions (Zhang and Hu 2001; Kraus et al., 2013; Zilberberg et al., 2018). Lohse et al. (2018) found a (relatively) simple way to probe four-dimensional quantum physical phenomena, starting from an artificial, two-dimensional dynamic system, a superlattice termed "2D topological charge pump". The light flowing through the two-dimensional superlattice behaves according to the predictions of the four-dimensional quantum Hall effect. The Authors provided a two-dimensional waveguide equipped with patterns acting as manifestations of higher-dimensional coordinates: in operational terms, they built a 2D lattice consisting of superlattices along the *x* and *y* axes. Each superlattice is achieved by superimposing two standing waves of different wavelength (**Figure 2A**). When a third wave is introduced along the *x* direction, this corresponds to tilting the long lattice along a one-dimensional path shadowing the axis x, carefully choosing the proper inclination (**Figure 2B**). Lohse et al. (2018) and Zilberberg et al. (2018) provided the proper measures (e.g., angles, equations) to detect the 4D quantum Hall effect. Their procedure on 2D topological charge pumps allows the achievement of dynamics along the y axis that are equivalent to movements in four spatial dimensions. They attained two different responses: a linear one (two-dimensional response) along the axis x and a nonlinear one (four-dimensional response) along the *y* axis (**Figure 2C**). In sum, the Authors provide a technique which describes quantum dynamics in terms of pure oscillations. Here we ask: could such procedure be transferred, with the due corrections, to quantum computing, in order to build a spatial four-dimensional device where quantum computational operations might take place?

Computations in the form of shape maps. In the previous paragraph, we showed thay Lohse et al.'s (2018) approach, i.e., a 2D topological charge pump, holds true for the assessment of the unusual multidimensional phenomenon occurring in quantum dynamics' Hall effect. Here we aim to show how, with the proper amendments, their four-dimensional- apparatus could be also used to build, assess and quantify a further spatial dimension of quantum computers endowed in two-dimensional lattices. In other terms, our aim is to explore 4D shapes using 2D functional lattices, where the constructing basis in the x and the y dimensions are superlattices, i.e., periodic layered structures derived from the superposition of two stationary waves of different wavelengths. Our goal is to correlate shape maps to Lohse' et al.'s 2D lattice oscillations, the latter standing for the S_0 at the Oth level of synthesis (**Figure 3, lowest part**). The entire topological pump stands for the space K, while its horizontal and vertical oscillations stand, respectively, for $A, B \subset K$. The topological pump's phase φ_x (which is the pump parameter, achieved when pumping is performed by moving the long lattice along x) stands for the probe function φ_1 displayed in **Figure 1A**. The topological pump's phase φ_y (which stands for a transverse superlattice phase that depends linearly on x, and which varies with φ_x changes) stands for the probe function φ_2. Note that φ_x lies at the S_1 level of synthesis, while φ_y at the S_2 level. In sum, when φ_x is modified, we achieve changes in φ_y, which lead to a quantized non-linear response along y: such nonlinear response stands for the four-dimensional features in the topological space K. Note that, when an adiabatic pump cycle of the 2D topological charge pump is performed (**Figure 4**), we achieve periodic modulation along closed trajectories, both on the horizontal and vertical plane (curves φ_x and φ_x **in the upper part of the Figure 4**). In a full pump cycle, these closed trajectories cover a closed surface which lies in the 4D parameter space (**middle part of Figure 4**).

Hyper-BUT. Although optical computing architectures use classical superposition of electromagnetic waves, they are not able to assess specific quantum mechanical phenomena such as entanglement. Therefore, they have lower potential for computational speed-up than the proper quantum computers. In turn, although our 2D topological charge pump may be defined as an optical computer, the availability of a fourth spatial dimension overturns the above-mentioned limitation. Indeed, our model allows the assessment of antipodal points in higher dimensions, due to the hyper-BUT dictates (**Figure 4, lower part**). When evaluating 2D signals in 4D phase spaces, we achieve a

multidimensional structure equipped with antipodal features with matching description, in touch with Peters and Tozzi (2016), who suggested quantum entanglement as occurring in four spatial dimensions.

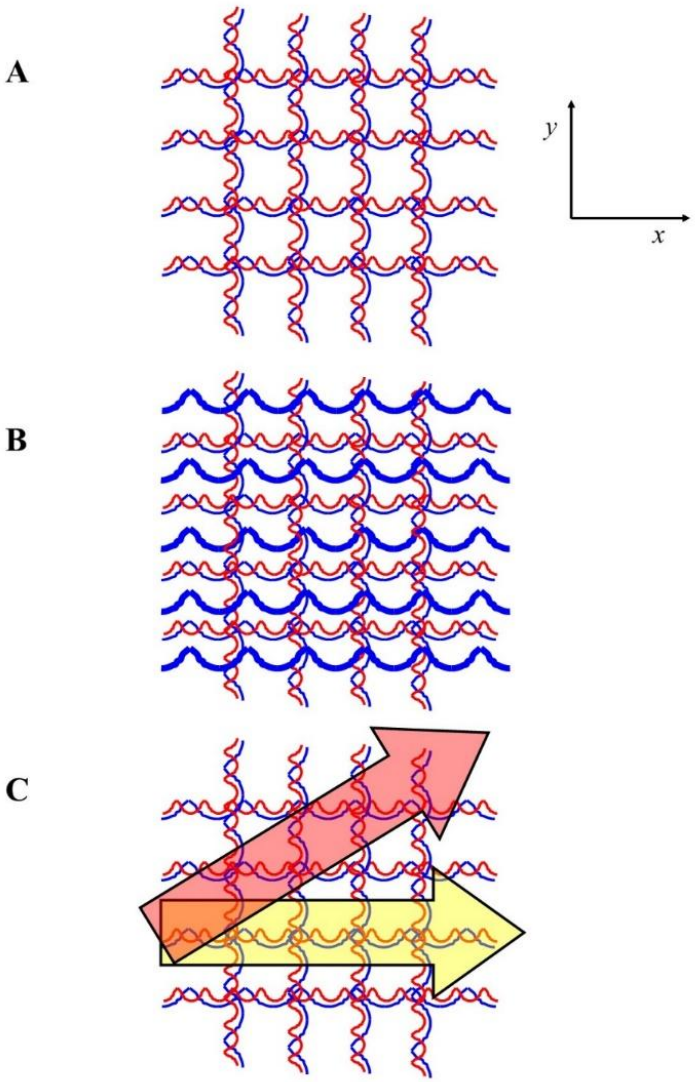

Figure 2. 4D physical activities on a 2D superlattice, according to Lohse et al. (2018). **Figure 2A** illustrates a topological lattice with two waves of different wavelength (red and blue thin lines). **Figure 2B** depicts a third wave (blue thick line) with the proper wavelength and angulation (not shown here) superimposed to the lattice along the x direction. The required angulation of the third wave might also be achieved by tilting the lattice. **Figure 2C**: the superimposition of the three waves gives rise to two different paths: a 2D linear one along the x axis (yellow arrow), and a nonlinear 4D one along the y axis (red arrow). Modified from Tozzi (2019).

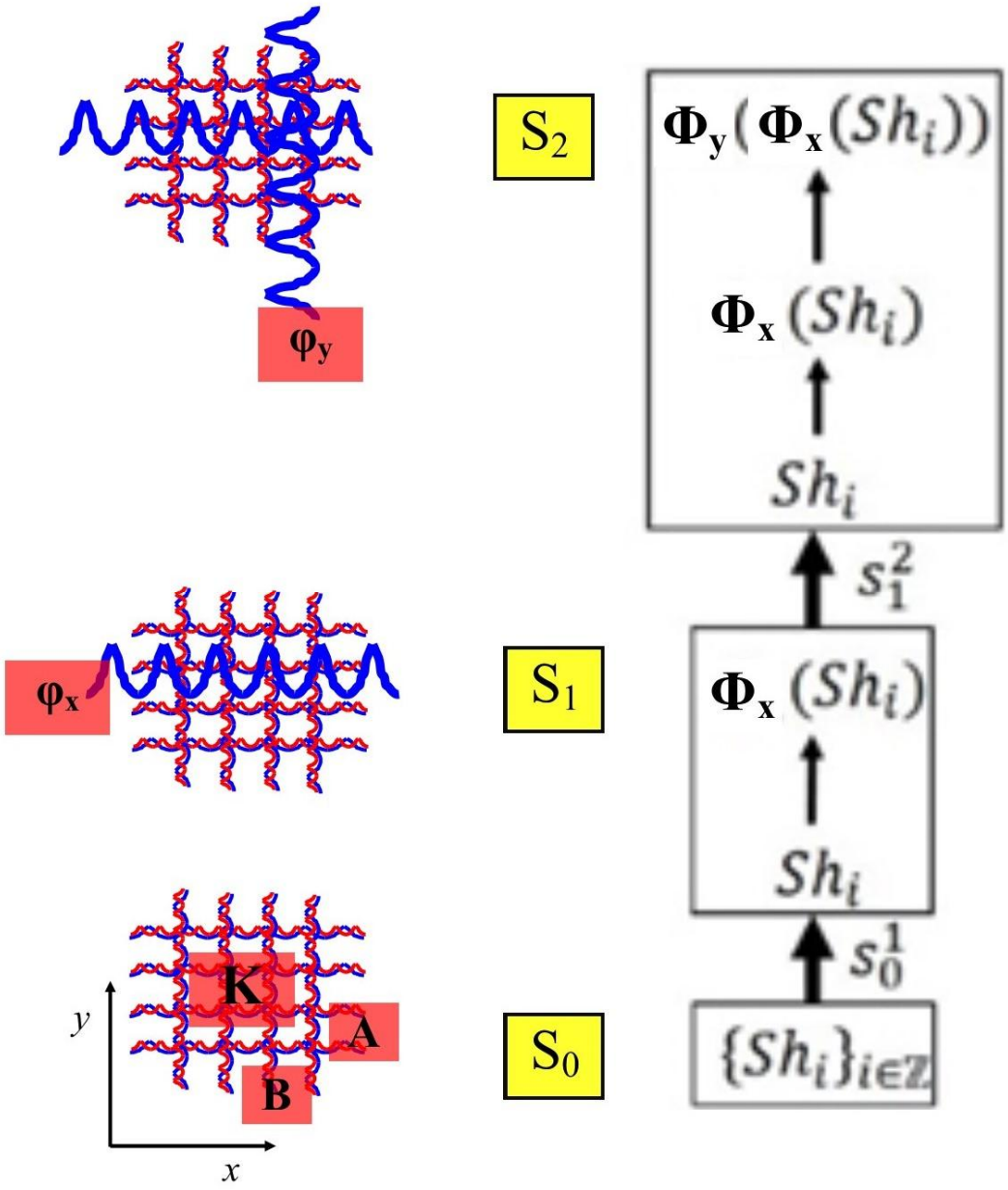

Figure 3. Near set theory's and shape maps' lexicon can be used to describe the operations taking place on the 2D topological charge pump too. The yellow squares describe the levels of synthesis, while the red ones the near set theory's counterparts of the Lohse et al.'s lattice.

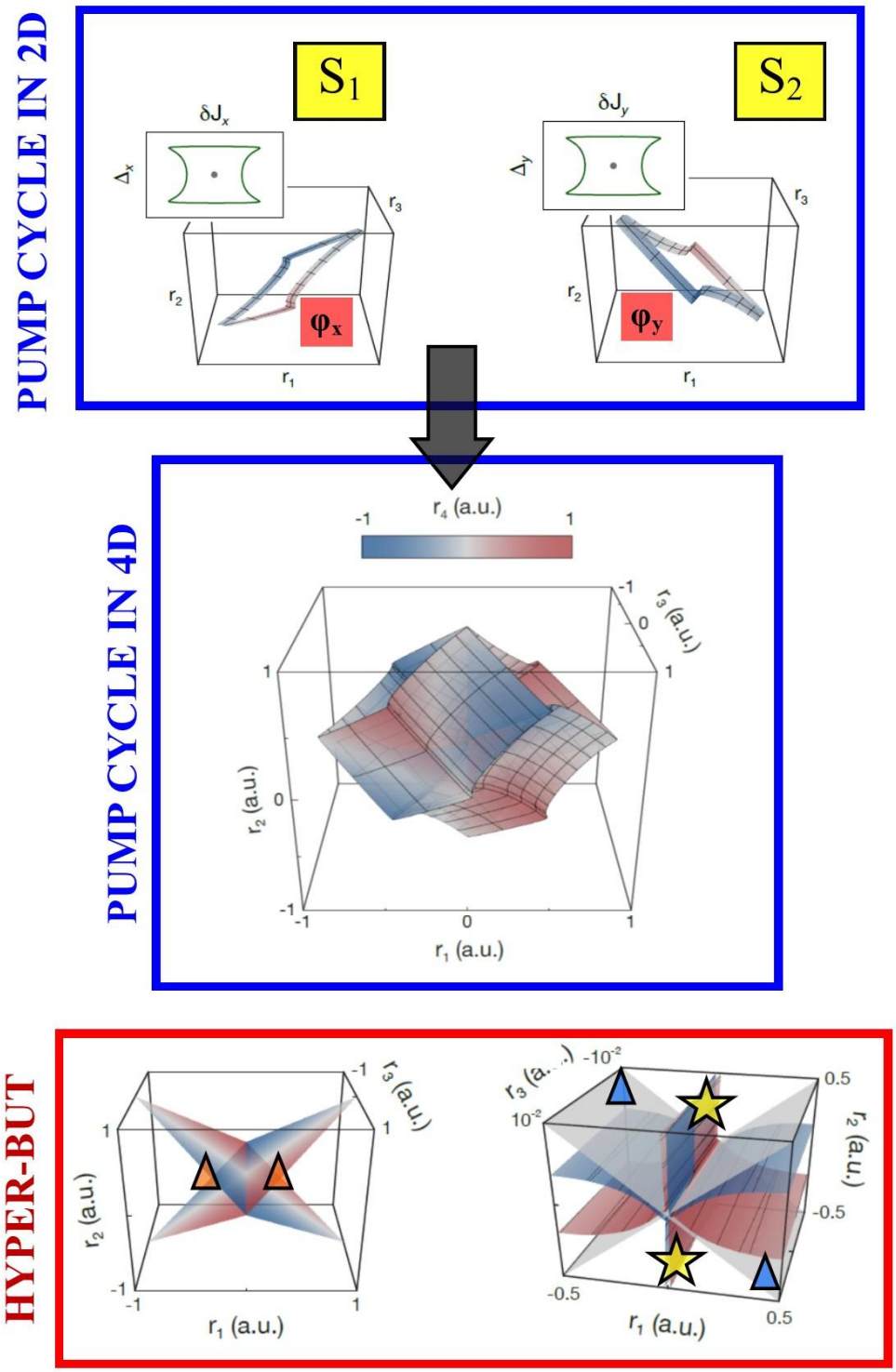

Figure 4. Adiabatic pump cycle in different dimensions. Note that the paths in 2D give rise to a multifaceted manifold in 4D. The lower part of the Figure (embedded in a red square) illustrates how the Borsuk-Ulam theorem holds true for the 2D topological charge pump. Indeed, inside the transformed parameter space where singularities correspond

to planes that touch at the origin, it is easy to detect several antipodal points with matching description (green and blue triangles, yellow stars). See Lohse et al. (2018) for further details and the legenda of the plots depicted here.

CONCLUSIONS

We aimed to transfer the framework of the quantum Hall effect provided by Lohse et al. (2018) to the realm of quantum computation, in order to: a) describe real multidimensional mathematical/physical/biological dynamics and b) demonstrate the feasibility of a synthetic network equipped with four spatial dimensions (plus time), instead of the classical three (plus time). We provide the theoretical apparatus to link 2D topological charge pump to topological shape maps, achieving quantum computing in four spatial dimensions. Indeed, working on a properly manipulated two-dimensional quantum lattice such as the 2D topological charge pump, it is feasible to build a transverse oscillation standing for the whole system's four-dimensional component. We showed how the superimposition of waves of different frequency and orientation produces the required superlattice's functional reticulum. When the latter is crossed by other waves of different frequency along its x axis, both (two-dimensional) linear and (four-dimensional) nonlinear dynamics are accomplished. The superimposition of the proper waves gives rise to two quantifiable and assessable different motions: a linear one along the x axis, and a nonlinear one along the y axis. The oscillatory response along the y axis stands for the artificial network's component displaying the fourth spatial dimension.
The question is: why might scientist perform computations in four spatial dimensions, instead of the canonical three? How much could quantum computing profit from operations taking place in higher dimensions? When projecting qbits from lower to higher dimensions, their number increases, due to the dictates of the recently-developed variants of the Borsuk-Ulam theorem (Tozzi and Peters, 2016b). Taking into account our framework, the shape projection from two to four spatial dimensions allows to achieve FOUR shapes with matching description, because the mappings takes place two dimensions higher. This means that a 4D quantum computer (built on an easily manageable 2D lattice) amplifies four times the same message (which can be described in terms of qbits), but does not require increases in phase space's volume: indeed, going in higher dimensions, the manifold volume does not increase, while the information does. In other words, the interaction among different waves produces a novel functional dimension, i.e., a higher dimensional phase space where computational operations take place more efficiently at the same energetic cost.
To provide a theoretical operational example, in a visual 2D scene the presence of the shape causes a deformation in 2D topological charge pumps. The resulting 4D wave stands for the computer's response to the introduction of the object in its oscillatory lattice. Therefore, 4D oscillation is the main feature that multiplies the number of shapes. Further, the x and y axes can be arranged in varying orientations according to different required shape reconstructions, allowing to increase discriminatory power and detectable features. Also, the fourth dimension overtakes one of the current limitations of optical quantum computing, i.e, the impossibility to achieve quantum entanglement. Indeed, entangles particles, hidden in lower dimensions, are detectable in higher ones, as demonstrated by Peters and Tozzi (2016). The last, but not the least, different mathematical/physical/biological activities might exhibit different four-dimensional hidden components, that, once detected, could be experimentally assessed and quantified.

REFERENCES

1) Ahmad MZ, Peters JF. 2018. Descriptive unions. A fibre bundle characterization of the union of descriptively near sets, arXiv 1811, no. 11129, 1-19.
2) Borsuk K. 1957-58. Concerning the classification of topological spaces from the standpoint of the theory of retracts, XLVI, 177–190.
3) Di Concilio A, Guadagni C, Peters JF, Ramanna S. 2018. Descriptive proximities. Properties and interplay between classical proximities and overlap. Mathematics in Computer Science 12, no. 1, 91-106.
4) Dmochowski JP, Ki JJ, DeGuzman P, Sajda P, Parra LC. 2017. Extracting multidimensional stimulus-response correlations using hybrid encoding-decoding of neural activity. Neuroimage. 2017 May 22. pii: S1053-8119(17)30429-9. doi: 10.1016/j.neuroimage.2017.05.037.

5) Garcia JO, Ashourvan A, Muldoon SF, Vettel J, Bassett DS. 2018. Applications of Community Detection Techniques to Brain Graphs: Algorithmic Considerations and Implications for Neural Function. Proceedings of the IEEE PP(99):1-22. DOI10.1109/JPROC.2017.2786710.
6) Hall E. 1879. On a New Action of the Magnet on Electric Currents. American Journal of Mathematics. 2 (3): 287–92. doi:10.2307/2369245.
7) Kraus YE, Ringel Z, Zilberberg, O. 2013. Four-dimensional quantum Hall effect in a two-dimensional quasicrystal. Phys. Rev. Lett. 111, 226401.
8) Lohse M, Schweizer C, Price HM, Zilberberg O, Bloch I. 2018. Exploring 4D quantum Hall physics with a 2D topological charge pump. Nature 553, 55–58. doi:10.1038/nature25000.
9) Matoušek J. 2003. Using the Borsuk–Ulam Theorem. Lectures on Topological Methods in Combinatorics and Geometry. Springer-Verlag Berlin Heidelberg, 2003
10) Novoselov KS, Jiang Z, Zhang Y, Morozov SV; Stormer HL, et al. 2007). Room-temperature quantum Hall effect in graphene. Science. 315 (5817): 1379.
11) Peters JF. 2007. Near sets. Special theory about nearness of objects. Fundamenta Informaticae 75, nos. 1-4, 407-433.
12) Peters JF. 2014. Topology of Digital Images. Visual Pattern Discovery in Proximity Spaces, Intelligent Systems Reference Library, vol. 63, Springer, ISBN 978-3-642-53844-5, pp. 1-342.
13) Peters JF, Tozzi A. 2016. Quantum Entanglement on a Hypersphere. Int J Theoret Phys, 1–8. doi:10.1007/s10773-016-2998-7.
14) Tozzi A, Peters JF. 2016a. Towards a Fourth Spatial Dimension of Brain Activity. Cognitive Neurodynamics 10 (3): 189–199. doi:10.1007/s11571-016-9379-z.
15) Tozzi A, Peters JF. 2016b. A Topological Approach Unveils System Invariances and Broken Symmetries in the Brain. Journal of Neuroscience Research 94 (5): 351–65. doi:10.1002/jnr.23720.
16) Tozzi A, Peters JF, Fingelkurts AA, Fingelkurts AA, Marijuán PC. 2017. Topodynamics of metastable brains. Physics of Life Reviews, 21, 1-20. http://dx.doi.org/10.1016/j.plrev.2017.03.001.
17) Tozzi A. 2019. The multidimensional brain. Physics of Life Reviews. doi: https://doi.org/10.1016/j.plrev.2018.12.004. In press.
18) Zhang, S-C, Hu J. 2001. A four-dimensional generalization of the quantum Hall effect. Science 294, 823–828.
19) Zilberberg O, Huang S, Guglielmon J, Wang M, Chen KP, et al. 2018. Photonic topological boundary pumping as a probe of 4D quantum Hall physics. Nature. 2018 Jan 3;553(7686):59-62. doi: 10.1038/nature25011.